HHS Public Access

Author manuscript

Hippocampus. Author manuscript; available in PMC 2017 September 01.

Published in final edited form as:

Hippocampus. 2016 September ; 26(9): 1124–1139. doi:10.1002/hipo.22595.

Oxytocin Depolarizes Fast-Spiking Hilar Interneurons and Induces GABA Release onto Mossy Cells of the Rat Dentate Gyrus

Scott W. Harden[1,2] and **Charles J. Frazier**[1,3]

[1]Department of Neuroscience, College of Medicine, University of Florida

[2]Department of Oral Biology, College of Dentistry, University of Florida

[3]Department of Pharmacodynamics, College of Pharmacy, University of Florida

Abstract

Delivery of exogenous oxytocin (OXT) to central oxytocin receptors (OXT-Rs) is currently being investigated as a potential treatment for conditions such as post-traumatic stress disorder (PTSD), depression, social anxiety, and autism spectrum disorder (ASD). Despite significant research implicating central OXT signaling in modulation of mood, affect, social behavior, and stress response, relatively little is known about the cellular and synaptic mechanisms underlying these complex actions, particularly in brain regions which express the OXT-R but lie outside of the hypothalamus (where OXT-synthesizing neurons reside). We report that bath application of low concentrations of the selective OXT-R agonist Thr4,Gly7-OXT (TGOT) reliably and robustly drives GABA release in the dentate gyrus in an action potential dependent manner. Additional experiments led to identification of a small subset of small hilar interneurons that are directly depolarized by acute application of TGOT. From a physiological perspective, TGOT-responsive hilar interneurons have high input resistance, rapid repolarization velocity during an action potential, and a robust afterhyperpolarization. Further, they fire irregularly (or stutter) in response to moderate depolarization, and fire quickly with minimal spike frequency accommodation in response to large current injections. From an anatomical perspective, TGOT responsive hilar interneurons have dense axonal arborizations in the hilus that were found close proximity with mossy cell somata and/or proximal dendrites, and also invade the granule cell layer. Further, they have primary dendrites that always extend into the granule cell layer, and sometimes have clear arborizations in the molecular layer. Overall, these data reveal a novel site of action for OXT in an important limbic circuit, and represent a significant step towards better understanding how endogenous OXT may modulate flow of information in hippocampal networks.

Keywords

hilus; electrophysiology; hippocampus; cellular neurophysiology; patch clamp

Corresponding Author (*): Charles J. Frazier, Ph.D., Associate Professor, University of Florida, Departments of Pharmacodynamics and Neuroscience, 1345 Center Drive, JHMHC Box 100487, Gainesville, FL 32610, USA, cjfraz@ufl.edu, Phone: 352-273-7686, Fax: 352-273-7705.

Introduction

Oxytocin (OXT) is an ancient neuropeptide (Beets et al., 2012; Grimmelikhuijzen and Hauser, 2012; Knobloch and Grinevich, 2014) synthesized by magnocellular neurons located in the paraventricular nucleus (PVN) and supraoptic nucleus (SON) of the hypothalamus (Grinevich et al., 2016; Knobloch and Grinevich, 2014). Several well-known peripheral effects of OXT (i.e., milk ejection and uterine contraction) depend on activity dependent release of OXT into the systemic circulation from magnocellular neurosecretory neurons, which occurs via axonal projections through the hypophyseal portal system to the posterior pituitary (Sivukhina and Jirikowski, 2016). However, oxytocinergic magnocellular neurosecretory neurons also send axonal projections to numerous extra-hypothalamic brain regions that express oxytocin receptor (OXT-R) including the entorhinal cortex, amygdala (medial and central), bed nucleus of the stria terminalis, septum (lateral and medial), and hippocampus (Dumais and Veenema, 2015; Hammock and Levitt, 2013; Insel and Shapiro, 1992; Ophir et al., 2012; Raggenbass et al., 1989). Further, these neurons are able to release peptide dendritically (Kombian et al., 1997; Leng et al., 2008; Ludwig and Pittman, 2003), creating local paracrine signals in the CNS, and possibly contribute to volume transmission via the ventricular system (Grinevich et al., 2016).

In recent years, it has become clear that centrally acting OXT is likely to modulate limbic function in ways that have profound impact on trust, fear, stress response, and other complex social behaviors (Hammock and Young, 2006; Johnson et al., 2015; Knobloch et al., 2012; Lee et al., 2009). Further, aberrant central OXT signaling has been associated with neurodevelopmental disorders such as autism spectrum disorder (Feldman et al., 2014; Lerer et al., 2008; Modahl et al., 1998; Taurines et al., 2014). Acute application of exogenous OXT (by blood infusion or intranasal application) provides transient relief from some ASD symptoms in humans (Anagnostou et al., 2014; Aoki et al., 2014; Hollander et al., 2007; Hollander et al., 2003; Watanabe et al., 2014; Watanabe et al., 2015) and when applied into the cerebroventricular system in animal models of ASD (Sala et al., 2011).

The hippocampal formation (HPF) is intimately involved in information processing in limbic circuits, and hippocampal impairment has been independently implicated in some neurodevelopmental disorders that are beginning to be associated with aberrant OXT signaling (Dager et al., 2007; Maister et al., 2013; Nicolson et al., 2006; Saitoh et al., 2001). Further, recent studies have revealed that acute OXT exposure improves hippocampal function in-vivo, and both depolarizes interneurons and enhances synaptic transmission in area CA1 in-vitro (Owen et al., 2013; Tomizawa et al., 2003; Zaninetti and Raggenbass, 2000).

The current study sought to reveal novel effects of OXT-R activation in the hilar region of the dentate gyrus, as this area plays a key role in gating flow of information into hippocampal networks (Hsu, 2007), undergoes extensive remodeling during early development (Danglot et al., 2006), possesses interneurons which express OXT-R (Oh et al., 2014; Tribollet et al., 1989), and yet has never been carefully evaluated in a way that reveals detailed cellular and synaptic effects of OXT-R activation. Our results reveal that OXT-R

activation robustly depolarizes a small subset of electrophysiologically and anatomically identifiable hilar interneurons which appear to provide local inhibition to hilar mossy cells.

Methods

Hippocampal slice preparation

Male Sprague Dawley rats (p14-p19) were used for this study. All procedures were approved by the University of Florida Institutional Animal Care and Use Committee (IACUC). All animals were housed with multiple littermates and their nursing mother. All electrophysiological studies were performed on brain slices prepared similarly to previous studies from this laboratory (Hofmann et al., 2011). Animals were anesthetized by ketamine injection (1 mL of 2% ketamine in sterile physiological saline via i.p. injection). Rats were decapitated and brains were rapidly extracted and horizontally sectioned to 300 μm using a Leica VT1000s vibratome while submerged in ice-cold sucrose-laden oxygenated artificial cerebrospinal fluid (ACSF) containing (in mM): 87 NaCl, 2.5 KCl, 1.25 NaH_2PO_4, 7 MgCl, 10 dextrose, 0.5 $CaCl_2$, 75 sucrose, and 25 $NaCHO_3$. The HPF was dissected from the rest of the brain and transferred to low-calcium ACSF containing (in mM): 124 NaCl, 2.5 KCl, 1.23 NaH_2PO_4, 10 dextrose, 1 $CaCl_2$, 3 $MgSO_4$, and 25 $NaCHO_3$ maintained at 37 °C in a hot water bath. After a 30-minute incubation, slices were removed from the water bath and permitted to passively equilibrate to room temperature over 30 minutes.

Electrophysiology and pharmacology

All live cell recordings were performed in a low turbulence perfusion chamber (JG-23W/HP, Warner Instruments) using infrared differential interference contrast (IR-DIC) microscopy with an Olympus BX51WI upright stereomicroscope, a 12-bit IRC CCD camera (QICAM Fast 1394, QImaging), and a 40x water immersion lens. Acute brain slices were continuously perfused with oxygenated ACSF at a rate of 1–2 mL/min. Patch pipettes were prepared with a Flaming/Brown-type pipette puller (Sutter instrument, P-97) from 1.5 mm / 0.8 mm borosilicate glass capillaries (Sutter instrument) and pulled to an open tip resistance of 4–10 MΩ. Recordings were made using a Multiclamp 700B amplifier, Digidata 1440A digitizer, and ClampEx 10.2 software (all Molecular Devices). Off line analysis of electrophysiological data was completed using custom software made by CJF or SWH in OriginC (Originlab, Northampton, MA) or Python 2.7 and the Neo 0.3.3 library (http://pythonhosted.org/neo/). Unless otherwise specified, all patch-clamp recordings were performed using ACSF containing (in mM) 126 NaCl, 11 dextrose, 1.5 $MgSO_4$, 3 KCl, 1.2 NaH_2PO_4, 1 EGTA, and 25 $NaHCO_3$ continuously oxygenated with 95% O_2 / 5% CO_2. Patch pipettes were filled with a potassium gluconate-based pipette solution containing (in mM) 10 KCl, 5 NaCl, 2 $MgCl_2$, 1 EGTA, 10 HEPES, 130 K-gluconate, 10 phosphocreatine, 2 Na_2-ATP, 0.3 Na-GTP, adjusted to pH 7.25 and 290 mOsm. To minimize effects of neurotransmitter release from adjacent neurons, most fast neurotransmission was blocked by pharmacologically inhibiting kainate receptors, AMPA receptors, NMDA receptors, $GABA_A$ receptors, $GABA_B$ receptors, and muscarinic acetylcholine (mACh) receptors with 20 μM DNQX, 40 μM AP5, 100 μM picrotoxin (PTX), 10 μM CGP-55845 (CGP), and 5 μM atropine, respectively (all bath-applied). All drugs were ordered from TOCRIS except PTX which was ordered from Sigma-Aldrich. Stock solutions for PTX and CGP were dissolved

in DMSO such that bath concentration never exceeded 0.1%, and did not change during application of OXT-R selective compounds. In experiments that measure inhibitory postsynaptic currents (IPSCs), cells were filled with a high [Cl^-] pipette solution containing (in mM): 140 KCl, 1 $MgCl_2$, 0.2 EGTA, 10 HEPES, 2 Na_2-ATP, 0.4 Na-GTP, and 4 NaCl adjusted to pH 7.25 and 290 mOsm, and PTX was omitted from the bath solution. All pipette solutions were filtered using a 0.22 micron filter and stored in 100 μL aliquots at −20 °C. OXT-R agonist Thr4,Gly7-OXT (TGOT, 0.1–0.2 μM), OXT-R antagonist (d(CH2)51,Tyr(Me)2,Thr4,Orn8,des-Gly-NH29)-vasotocin (dOVT, 1 μM), and tetrodotoxin (TTX, 1 μM) were dissolved in bath solution at 25–50x final concentration and applied via syringe pump at 0.4 mL/min to the perfusion line via an injection port. As a result, solutions were diluted to final concentration immediately before entering the recording chamber. Final bath concentrations are expected to closely match concentrations at the receptors, with the possible exception of TGOT, which is applied more briefly and is likely subject to enzymatic degradation by endogenous peptidases.

All voltage-clamp recordings where TGOT was applied were acquired continuously at 20 kHz in 10 second sweeps with no inter-sweep interval. The holding potential was −70 mV for mossy cells, and −50 mV for all other hilar interneurons. Each sweep was preceded by a 200 ms −10 mV voltage step to monitor membrane resistance, access resistance, and whole cell capacitance. Access resistance was carefully monitored in all voltage clamp experiments that quantified data from synaptic currents. For these experiments, cells were excluded from analysis if access resistance changed by ≥ 30% during the course of the experiment, or if abrupt changes in access were temporally associated with clear changes in frequency or amplitude of synaptic currents.

All neurons were characterized electrophysiologically using a standard set of protocols to assess current/voltage relationships and action potential firing properties. In voltage clamp configuration, neurons were stepped from −110 mv through −50 mV in 5 mV steps for 2 seconds (when recording from mossy cells) or 500 ms (for all other neurons). To minimize the influence of spontaneous currents in these measurements (especially when using a high [Cl^-] internal solution), steady state current was calculated from the peak of a Gaussian-fitted histogram of data samples which eliminated outliers (a strategy we have previously successfully used to separate GABA-mediated phasic currents from tonic currents (Nahir et al., 2007)). In current clamp configuration, action potential firing properties of all cells were assessed using 2 second current steps from −200 pA through +500 pA in 100 pA steps (when recording from mossy cells) or from −100 pA through +250 pA in 50 pA steps (for all other neurons). Steady state firing frequency was determined as the inverse of the average interspike interval from all APs in the last 50% of the current step. Accommodation was defined as the ratio of the instantaneous frequency of the first two action potentials (calculated as the inverse of the interspike interval) to the average steady state firing frequency. Action potential repolarization velocity was defined as the nadir of the first derivative of its voltage recording with respect to time (20 kHz sample rate). Action potential threshold was calculated as the voltage at which the depolarization velocity exceeded 5 mV/ms. Afterhyperpolarization (AHP) was calculated as the difference from the action potential threshold to the minimum voltage in the 25 ms following the action potential. Action potential half-width was measured as the time that the voltage exceeded the

value observed halfway between threshold and peak, similar to Hosp et al. (2014). Phase diagrams were made by plotting the first derivative of the membrane potential (action potential velocity) with respect to instantaneous voltage, similar to other studies (Bean, 2007; Burton and Urban, 2014; Elgueta et al., 2015; Lu et al., 2014).

Identification and characterization of mossy cells and other hilar interneurons

The hilar region of the dentate gyrus, also known as the polymorphic cell layer, is a region encircled by the granule cell layer, and excluding CA3 pyramidal cells. For the initial experiments in this study, it was necessary to record from hilar mossy cells. Mossy cells are unique among all the local circuit neurons found in the hilus, and indeed in the hippocampus, in several respects. Perhaps most notably, they are large, glutamatergic local circuit neurons that tend to send axonal projections both along the septo-temporal axis of the hippocampus, and across the hippocampal commissure (Scharfman and Myers, 2013). They receive robust excitatory synaptic input via large proximal dendritic spines, are very sensitive to hypoxia/excitotoxicity, and are strongly implicated in several models of epileptogenesis (Sloviter 1991, Scharfman, 1994; Seress et al., 2009).

Putative mossy cells were identified using techniques similar to those previously described by our laboratory (Nahir et al., 2007; Hofmann and Frazier, 2010; Lindsly and Frazier, 2010). Briefly, mossy cells were initially targeted using IR-DIC microscopy (Fig. 1a, 1b). Targeted cells had a large soma (typically 15–30 μm in diameter) located in the hilus. The presence multiple thick primary dendritic branches tend to give these cells a unique large rhomboidal shape under IR-DIC.

Following establishment of whole-cell patch-clamp configuration, putative mossy cells were further identified by multiple electrophysiological parameters. In the current study, mossy cells had a characteristically large whole cell capacitance (137.63 ± 9.67 pF, n=26), and featured a robust hyperpolarization-activated, slowly activating, slowly inactivating excitatory current. In current clamp configuration, this feature is visible as a “sag” in response to a hyperpolarizing current pulse (Fig. 1e, left arrow) which is accompanied by depolarization which lasts several seconds following cessation of the current pulse (Fig. 1e, right arrow). Both of these features are observed in voltage-clamp configuration via the current response to a series of voltage steps (Fig 1f, left arrow and right arrow, respectively). Voltage-dependent conductances were measured in mossy cells and reported alongside those of non-mossy hilar interneurons for comparison (Fig. 1g–j). The prominent hyperpolarization activated excitatory current in mossy cells contributed to notably lower membrane resistance, particularly at negative potentials (Fig. 1g–h). Mossy cells also demonstrate an accommodating firing pattern in response to depolarizing current pulses (Fig. 1e) resulting in a slow (< 30Hz) steady state firing frequency which is often less than half of the initial firing frequency. As a result, mossy cells reach maximum firing frequency in response to moderate depolarizations (Fig. 1i), and display prominent accommodation (reported as the ratio of the instantaneous firing frequency of the first two action potentials to the average steady state firing frequency over the second half of the depolarization step, Fig. 1j).

After whole cell recording, fluorescent anatomical observations that relied on biocytin labeling of neurons (see next section) further revealed their extended axonal and dendritic architecture of recorded cells. Cells identified as mossy cells uniformly had characteristically large thorny excrescences ("moss") on their proximal dendrites (Fig. 1c), possessed numerous, large, highly branching dendrites confined to the hilus (Fig. 1d), and axonal projections which could often be observed exiting the hilus.

Biocytin labeling, immunohistochemistry, and fluorescent imaging

To assess detailed structural morphology of electrophysiologically-characterized neurons, pipette solution was supplemented with 5 mM biocytin. TGOT responsive hilar interneurons which were stable throughout all electrophysiological experiments were selected for detailed morphological analysis. The pipette was slowly retracted diagonally, and the integrity of the TGOT responsive hilar interneuron was verified under DIC optics (observed as a soma which remained largely unmoved throughout the experiment, and presented with the same morphology as it did before establishment of whole-cell configuration). Slices were transferred to 10% formalin and fixed overnight at 4 °C. Slices were then transferred into phosphate-buffered saline (PBS, pH 7.2) and stored at 4 °C until further processing. All subsequent histological labeling procedures were performed in a 12-well plate (1 mL reaction solution per well) at room temperature on an orbital shaker. Slices were washed (5 × 5min) with PBS with 0.1% Triton X-100 (PBST). Slices were then permeabilized for 24–48hr in a blocking solution (2% bovine serum albumin, 2% normal goat serum, and 0.1% NaN_3 in PBST). Slices were reacted with Alexa Fluor 594-conjugated streptavidin (ThermoFisher S-32356, 1:1000 in PBST) for 24 hours.

Immunohistochemical labeling of CCK and PV was performed on some TGOT responsive hilar interneurons which had been filled with biocytin. To minimize crossover of cell-fill fluorophore emission into the emission range used to image immunolabeled structures, tissues analyzed immunohistochemically were treated with Alexa Fluor 647-conjugated streptavidin in combination with secondary antibodies with lower wavelength fluorophores (Alexa Fluor 488 or 594). To further reduce spectral crossover, the concentration of biocytin was reduced from 5 mM to 250 nM. Together these changes promoted spectral separation of both fluorophores, but resulted in relatively weak biocytin labeling which only prominently labeled the TGOT responsive hilar interneuron soma and proximal structures, preventing detailed morphological analysis of extended axonal and dendritic morphology. Methods were similar to those for biocytin labeling alone, except for the inclusion of additional primary antibody incubation steps following the permeabilization step. Primary antibodies were applied in blocking solution for 48 hours (1:1000 mouse anti-CCK 8 (Abcam ab37274) or 1:1000 mouse anti-PV (Sigma-Aldrich P3088)) followed by a 5 × 5 minute washes in PBST. Secondary antibodies (1:500 goat anti-mouse) were applied in parallel with fluorophore-conjugated streptavidin for 24 hours.

Slices were washed with PBS (5 × 5 min), transferred to glass slides, and coverslipped with vectashield antifade mounting medium (H-1000). Fluorescent imaging was performed using an upright epifluorescence microscope with a 10x or 20x air objective lens using either an

X-cite 120Q arc lamp in combination with a CCD camera, or a two-photon femtosecond laser (810 nm) in combination with a photomultiplier tube.

Results

OXT-R activation causes action potential dependent release of GABA onto hilar mossy cells

Hilar mossy cells were voltage clamped at −70 mV using a high [Cl^-] pipette solution, resulting in an outward driving force on Cl^-. $GABA_B$, AMPA, NMDA, kainate, and mACh receptors were all blocked by bath application of appropriate concentrations of selective antagonists (see methods). Under these conditions, we observed that 3 minute bath application of 200 nM TGOT (selective OXT-R agonist with over 100,000 fold specificity for OXT-R over vasopressin (VP) receptor (Muhlethaler et al., 1983)) produced a robust increase in sIPSC frequency and amplitude that returned to baseline levels within 10 minutes (Fig. 2a). On average, this exposure to TGOT transiently increased sIPSC frequency (as measured from the 2–3 minute period following exposure) by 15.62 ± 3.80 Hz ($p < 0.01$, n=8) (Fig. 2c, blue trace). Similarly, sIPSC amplitude was significantly increased (by 9.04 ± 3.10 pA, $p < 0.05$, n=6). (Fig. 2e, blue trace). Both of these effects of TGOT were eliminated when the experiment was repeated in the presence of selective OXT-R antagonist dOVT (1 μM, n=4, Fig. 2c, e). Similarly, prior exposure to 1 μM TTX also eliminated the effects of bath applied TGOT on sIPSC frequency and amplitude (n=5, not illustrated). Fig. 2f illustrates the average sIPSC from a representative cell both before (n=577) and immediately after (n=707) application of 200 nM TGOT. Normalization of these traces to their peak amplitude revealed that TGOT had no effect on sIPSC kinetics (Fig. 2g).

Identification and intrinsic properties of putative TGOT responsive hilar interneurons

We next sought to identify GABAergic hilar neurons activated by TGOT, as such neurons would presumably contribute to TGOT mediated increases in sIPSC frequency observed in hilar mossy cells. In initial experiments, we simply targeted small hilar neurons under IR-DIC, recorded their basic electrophysiological properties, and then evaluated the effects of acute application of 0.1 – 1 μM TGOT in current or voltage clamp using whole cell recordings with a K-gluconate based internal solution (see Methods). Using this approach, we found very few hilar neurons that were directly depolarized by bath application of TGOT. After numerous trials it became clear that TGOT responsive neurons were likely to fire intermittently under moderate load. Therefore, we gradually began to intentionally target very small hilar neurons and test for the presence of this stuttering firing pattern before challenging with TGOT. This approach dramatically increased our success rate in finding TGOT responsive hilar neurons. Indeed, of 250 small hilar interneurons targeted during this project, only 57 (23%) were stuttering hilar interneurons which were then challenged with TGOT. Of those 57 cells, 40 (70%) exhibited an excitatory response to TGOT in either current or voltage clamp.

We sought to more rigorously characterize stuttering hilar interneurons which had a high probability of being TGOT responsive. This population of hilar interneurons is found in the deep hilus (Fig. 3a, arrow), often in close approximation with putative mossy cells (Fig. 3a,

asterisks). Putative TGOT responsive hilar interneurons had relatively small soma (typically smaller than 10 μM) and were markedly circular or ovoid when viewed with DIC optics (Fig. 3a, arrow). In voltage clamp configuration, voltage steps revealed a hyperpolarization activated excitatory current which, compared to the hyperpolarization activated current in mossy cells, was quick to activate and deactivate (Fig. 3b, arrows). This feature was also observed in response to current steps in current-clamp configuration as a “sag” in response to a hyperpolarizing pulse, with no persistent excitatory current once the pulse terminates (Fig. 3c, arrows). Depolarizing steps revealed subthreshold, perithreshold oscillations (Fig. 3c). TTX-sensitive perithreshold oscillations have been reported in other hippocampal interneuron populations (Chapman and Lacaille, 1999), and similarly we observed perithreshold oscillations in putative TGOT responsive hilar interneurons were eliminated in the presence of TTX (data not shown). Strong current injection (+250 pA) in putative TGOT responsive hilar interneurons induced maximal steady-state firing frequency that was always in excess of 30 Hz, with generally little spike frequency accommodation. Further, putative TGOT responsive hilar interneurons consistently demonstrated a prominent AHP after each action potential (Fig. 3d), had a small action potential half-width (Fig. 3e), and rapid repolarization velocity (observed by inspecting the first derivative of the membrane potential) (Fig. 3f). These two traces were combined to form of a phase diagram (Lu et al., 2014) with a shape characteristic of putative TGOT responsive hilar interneurons (Fig. 3g). Collectively, these features were used to classify putative TGOT responsive hilar interneurons as small, non-accommodating, fast spiking hilar interneurons, that would fire intermittently (or stutter) under moderate load.

Effects of OXT-R activation in TGOT responsive hilar interneurons

As noted above, only 57 of 250 small hilar neurons tested met criteria (as described above) to be categorized as putatively TGOT responsive. Of 57 putative TGOT responsive hilar interneurons, 40 responded to acute application of TGOT (with a sigmoidal drug response which reached maximum effect 2–3 minutes after TGOT application and then began to recover toward baseline) and thus were categorized as TGOT responsive hilar interneurons. In current clamp configuration, TGOT responses were observed as transient depolarizations that resulted in clear increases in action potential frequency (Fig. 4a,b). On average, acute application of TGOT increased firing rate in TGOT responsive hilar interneurons by 3.96 ± 037 Hz ($p < 0.001$, n=6) in response to this exposure (Fig. 4b). In voltage-clamp configuration, identical application of TGOT produced a large inward current (21.73 ± 2.90 pA, n=25, $p<0.001$, Fig. 1j, Fig. 4c, blue trace). Interestingly, the excitatory effect of TGOT in TGOT responsive hilar interneurons, whether observed in current clamp or voltage clamp, had time dynamics similar to the changes in sIPSC frequency and amplitude observed in mossy cells (Fig. 2c,e). In sharp contrast, TGOT failed to have any significant effect on action potential frequency or holding current (in current or voltage clamp experiments, respectively) in a subset of cells (17 of 57) that met criteria described above to be defined as putative TGOT responsive hilar interneurons.

We next sought to confirm the specificity of TGOT for OXT-R in our experimental conditions by preventing the TGOT-mediated excitatory current by prior exposure to 1 μM dOVT, a selective OXT-R antagonist (Owen et al., 2013; Zaninetti and Raggenbass, 2000).

However, because not all putative TGOT responsive hilar interneurons turn out to be actually TGOT responsive, an experimental design that involves pre-treatment with a OXT-R antagonist is not ideal. To address this issue, the concentration and duration of TGOT exposure (100 nM and 3 min, respectively) was carefully selected to minimize desensitization often reported associated with OXT-R (Oh et al., 2014), and TGOT was applied twice to each neuron, with a 20 min inter-application interval. In every cell which initially responded to TGOT, subsequent application in this manner produced a large second response (−15.54 ± 1.19 pA (n=4), Fig. 4c, blue trace). When 1 μM dOVT was added to the ACSF between the first and second TGOT application, the second response was eliminated (0.44 ± 1.49 pA, n=4, p<.001 Fig. 4c, green trace). Finally, in order to eliminate the possibility that TGOT was activating OXT-R on other neurons to promote action potential dependent release of an unknown transmitter, we evaluated the effects of TGOT in the presence of 1 μM TTX. Our results indicated that TGOT-mediated excitatory currents in TGOT responsive hilar interneurons were unaltered in the presence of TTX (−15.52 ± 4.26 pA, n=3, p > 0.05) (Fig. 4e,f).

Detailed differences in intrinsic properties between TGOT responsive and TGOT unresponsive fast spiking hilar interneurons

Although the criteria for identification of putative TGOT responsive hilar neurons as described in Fig. 3 are quite specific, we found it notable that even when such stringent criteria were used we only obtained a 70% success rate in predicting which hilar interneurons would be excited by TGOT prior to actually applying it. Therefore, extensive post-hoc analyses were performed to carefully compare the current/voltage relationship, gain, and degree of spike frequency accommodation in TGOT-responsive vs. TGOT unresponsive hilar interneurons that all met criteria described in Figure 3. Note that all intrinsic membrane properties described here were calculated from electrophysiological data obtained prior to TGOT exposure. We found a significant difference in holding current at subthreshold potentials positive of −65 mV (Fig. 5B) suggesting that TGOT responsive hilar interneurons rest at a slightly higher membrane potential. Further, we noted that the maximum steady state firing frequency obtained during large current injections was substantially higher in TGOT responsive vs. TGOT unresponsive hilar interneurons (Fig. 5c), while interestingly, spike frequency accommodation (see Methods) was significantly less pronounced (Fig. 5e). These features are generally apparent on representative traces illustrated in Fig. 5A. Finally, while all putative TGOT responsive hilar interneurons presented with generally similar AP features (Fig. 3), a detailed analysis of fast action potential dynamics revealed several significant differences in TGOT responsive hilar interneurons vs. TGOT unresponsive hilar interneurons. Specifically, we found that in TGOT responsive hilar interneurons, the amplitude of the afterhyperpolarization was larger (20.06 ± .66 mV vs. 14.86 ± .95 mV p=.0001, Fig. 5e), the AP half width was smaller (1.16 ± .04 ms vs 1.52 ± .09 ms, P<.01, Fig. 5f), and the peak repolarization velocity was more rapid (−64 ± 3.35 mV/ms vs −46.35 ± 4.27 mV/ms, P<.01 Fig. 5g), when compared to TGOT unresponsive hilar interneurons.

Anatomical and immunohistochemical features of TGOT responsive hilar interneurons

Electrophysiologically characterized TGOT responsive hilar interneurons which had been filled with biocytin were histologically processed to fluorescently label their architecture (see Methods). All TGOT responsive hilar interneurons examined in this manner (n=6) demonstrated a dense network of varicose axons in the body of the hilus (Fig. 6c) with projections into the body of the granule cell layer (Fig. 6b). Dendrites (putatively identified by their large diameter compared to axons, lack of varicose structures, and presence of spines) were always observed extending to the granule cell layer and in some cases extending beyond the granule cell layer and into the molecular layer (3/6) (Fig. 6d). Initial efforts to immunohistochemically characterize TGOT responsive hilar interneurons suggest that at least a subset of these cells are not immunoreactive for either cholecystokinin (CCK) or parvalbumin (PV) (See supplemental Fig. S1). To assess the potential of TGOT responsive hilar interneurons to form synapses onto mossy cells, a two-step recording procedure was used in which multiple neurons were filled with high concentration of biocytin to facilitate imaging of their extended axonal and dendritic structures. First, a putative TGOT responsive hilar interneuron was targeted by its electrophysiological and morphological characteristics (Fig. 7b) and confirmed as a TGOT responsive hilar interneuron by a strong increase in action potential frequency in response to TGOT exposure (Fig. 7c, inset). Following careful retraction of the recording pipette, adjacent mossy cells were targeted by their morphology under DIC optics (Fig. 7a), and confirmed as such by their electrophysiological and morphological features. Following fluorescent processing, the resulting tissue was imaged with standard and/or two-photon based epifluorescence microscopy (Fig. 7c) and presented as a maximum all-in-focus projection (Fig. 7d). Using this approach, we observed putative en passant synapses between the varicose axons from TGOT responsive hilar interneurons and the soma or proximal dendrites of mossy cells (e.g. Fig. 7D, inset).

Discussion

In the current study, we report that bath application of low concentrations of the selective OXT-R agonist TGOT reliably and robustly drives GABA release in the dentate gyrus in an action potential dependent manner. This increased GABA release was associated with increased frequency and amplitude of sIPSCs recorded from hilar mossy cells. Further, both effects were blocked by dOVT (an OXT-R antagonist) and by TTX. Although previous physiological studies have demonstrated that OXT-R activation can drive GABA release in areas such as CA1 of the hippocampus and the central amygdala (Knobloch et al., 2012; Owen et al., 2013; Viviani et al., 2010; Zaninetti and Raggenbass, 2000), this is the first such report in the dentate gyrus. Based on these observations, a primary question was whether there exists a population of GABAergic hilar interneurons that both innervate mossy cells and are directly depolarized by OXT-R activation. After substantial additional effort, we have identified such a population of neurons. Indeed, we describe a population of small hilar interneurons that irregularly fire, or stutter, in response to moderate current injection, and fire rapidly in response to large current injection. These neurons also have a prominent AHP, a narrow action potential width, and a rapid repolarization velocity all of which contribute to a distinct action potential shape. We report that although only a minority of small hilar

interneurons meet the criteria of this detailed phenotype, a majority of the of the ones that do are directly depolarized beyond threshold for firing action potentials by acute bath application of 100 nM TGOT. Intriguingly, we also find that when small, stuttering, fast spiking hilar interneurons are divided post-hoc by their responsiveness to TGOT, more fine grained physiological differences become apparent. Perhaps most notably, TGOT responsive neurons in this population appear to rest slightly more positive, have a significantly higher maximum firing rate, and are much less subject to spike frequency accommodation, while also having a significantly larger after hyperpolarization, narrower AP half width, and faster repolarization velocity. Additionally, anatomical studies presented here indicate that TGOT responsive hilar interneurons have dense axonal arborizations in the hilus that are often in close proximity with mossy cell somata and/or proximal dendrites, and yet also invade the granule cell layer. Further, they have primary dendrites that always extend into the granule cell layer, and sometimes have clear arborizations in the molecular layer. Finally, initial immunohistochemical studies indicate that these neurons do not display clear or consistent immunoreactivity for CCK or PV.

Overall, these results contribute substantially to a first careful characterization of a very small population of OXT-sensitive interneurons in the hilar region of the dentate gyrus, and provide significant insight into the likely physiological impact of endogenous OXT signaling in an important limbic area. In considering these data, it is important to highlight that the current studies were conducted on male rats age p14–19, and yet central OXT-R expression is known to be dynamic and may vary across age (Hammock and Levitt, 2013; Tribollet et al., 1989), species (Freeman et al., 2014; Olazabal and Young, 2006; Raggenbass et al., 1989), gender (Dumais and Veenema, 2015; Insel and Hulihan, 1995; Steinman et al., 2015), and even experience (Lukas et al., 2010; Prounis et al., 2015). As such, current data do not allow for strong or confident predictions about the extent to which OXT signaling in the dentate gyrus is affected by such variables. Nevertheless, we believe these data will also likely contribute to our understanding of potentially common mechanisms through which central OXT-R dependent signaling modulates CNS physiology. Toward this end, we believe there are a couple of additional topics on the specific experiments and data presented here that are worthy of more careful consideration.

First, with respect to effects of TGOT on sIPSCs recorded from hilar mossy cells, in the simplest sense we would have expected TGOT mediated depolarization of nearby interneurons to produce clear increases in sIPSC frequency, but not amplitude. In attempting to understand the mechanism through which sIPSC amplitude is also potentiated, we believe we can largely rule out postsynaptic effects on $GABA_A$ receptor conductance or expression, or other alterations in postsynaptic membrane resistance or active transport mechanisms, because acute application of TGOT does not similarly increase the amplitude (or frequency) of miniature IPSCs recorded in the presence of 1 μM TTX. One possible presynaptic mechanism for producing action potential dependent increases in sIPSC amplitude is through frequency-dependent facilitation, leading to calcium dependent increases in quantal content. While glutamatergic hippocampal pyramidal cells display robust synaptic facilitation (Chamberland et al., 2014), we believe this mechanism is unlikely to contribute to our results because fast-spiking inhibitory interneurons in general have low quantal content, and relatively high initial release probability, and as such are more likely to produce

frequency dependent depression than facilitation (Larimer and Strowbridge, 2008; Lindsly and Frazier, 2010; Owen et al., 2013). In our opinion, a more likely possibility is that TGOT enhances sIPSC amplitude in our experiments because it preferentially increases or initiates firing in a population of hilar neurons that selectively innervate mossy cell somata and proximal dendrites. Previous studies have indicated that some GABAergic hilar neurons do indeed preferentially target mossy cells at perisomatic locations (Acsady et al., 2000; Larimer and Strowbridge, 2008), and this hypothesis is also consistent with our own anatomical data on TGOT responsive neurons presented here. Further, a similar mechanism was theorized to underlie TGOT-mediated increases in sIPSC amplitude observed in CA1 pyramidal neurons, as described by (Zaninetti and Raggenbass, 2000) and further supported morphologically by (Owen et al., 2013).

Second, the use of immunohistochemical approaches to identify the neurochemical phenotype in TGOT responsive hilar interneurons is worthy of some additional considerations. Immunohistochemical description of TGOT-responsive hilar interneurons is desirable, because the combination of electrophysiological and morphological features observed here does not easily categorize them into any single existing class of hilar interneurons that has been previously described in the literature (e.g. see Freund and Buzsaki, 1996; Hosp et al., 2014; Lubke et al., 1998; Mott et al., 1997; Spruston et al., 1997). Previous work has demonstrated that CCK- and PV-expressing fast-spiking interneurons monosynaptically release GABA onto principal neurons of the HPF (Bartos and Elgueta, 2012), including mossy cells (Acsády et al., 2000). Of these, Acsády et al. (2000) suggested that CCK neurons were more likely to provide perisomatic innervation of mossy cells, which in combination with the effect on sIPSC amplitude discussed above, suggested the possibility that TGOT responsive hilar interneurons may express CCK. On the other hand, Owen et al. (2013), demonstrated that optogenetic activation of PV-expressing fast-spiking interneurons in CA1 (using a PV-Cre transgenic mouse line) closely mimicked TGOT-mediated changes in GABA signaling observed in hippocampal pyramidal cells. Nevertheless, our own immunohistochemical data (Supplemental Fig. 1) suggests that at least a subset of TGOT responsive hilar interneurons are not immunoreactive for CCK or PV. The lack of immunoreactivity observed here could potentially be explained if PV or CCK were dialyzed out of the cell during whole cell recording. Alternatively, cytoplasmic loading of biocytin may have resulted in masked immunoreactivity (a phenomenon Scharfman et al. (1989) has demonstrated occurs in hippocampal interneurons).. To overcome any immunohistochemical challenges related to cytoplasmic dialysis, future studies using cell-attached or loose-cell recordings to facilitate electrophoretic loading of biocytin while minimally disrupting the intracellular milieu (Joshi and Hawken, 2006) may be of use. However, it is important to note that in addition to CCK and PV, there also exist irregular firing hilar interneurons which express choline acetyltransferase (ChAT), vasoactive intestinal peptide (VIP), neuropeptide Y (NPY), somatostatin (SOM/SST), calbindin (CB), and calretinin (CR) (Fu and van den Pol, 2007; Porter et al., 1998; Savanthrapadian et al., 2014; Tepper et al., 2010; von Engelhardt et al., 2007). Thus, immunohistochemical labeling of additional protein markers, or single cell RT-PCR performed on carefully extracted cytoplasm may ultimately be necessary to reveal the complex neurochemical phenotype(s) of TGOT responsive hilar interneurons.

Third and more broadly, the mechanism of TGOT mediated depolarization, the phenotype of the underlying receptor, and the identity and availability of the endogenous agonist are also interesting topics to consider. In brief, if the mechanism of depolarization in TGOT responsive hilar interneurons is similar to the few published precedents (Gravati et al., 2010), future studies may find that TGOT mediated depolarization of hilar interneurons involves raised intracellular calcium and increased sodium permeability mediated by $G_q/11$ activation of an inositol 1,4,5-trisphosphate / diacyl glycerol signaling cascade. In terms of the underlying receptor, we believe the data presented here makes a strong case that the reported effects of TGOT in the hilus are in fact mediated by activation of OXT-Rs. Indeed, TGOT, the OXT-R agonist employed in our experiments, demonstrates selectivity for OXT-R over VP receptors that is greater than 100,000:1 (Muhlethaler et al., 1983). Similarly, the possibility that TGOT is acting off target at a non-OXT or VP receptor seems remote due to the fact that our effects were completely eliminated by the OXT-R antagonist dOVT at a concentration commonly employed in other studies (e.g. Owen et al., 2013). With regard to the endogenous agonist, we believe it is very likely that endogenous OXT ultimately leads to activation OXT-Rs on hilar interneurons and modulation of GABA release in the dentate gyrus similar to that demonstrated here. That said, it should be noted that OXT-Rs are known to be partially activated by VP (Gimpl and Fahrenholz, 2001; Gravati et al., 2010; Manning et al., 2012; Stoop, 2012), that VP-immunoreactive axons, as well as OXT-reactive axons, are also observed in the hilus of rats (Knobloch et al., 2012; Zhang and Hernandez, 2013), and that VP, as well as OXT, is present in the CSF at physiologically relevant concentrations in humans (Carson et al., 2015a; Carson et al., 2015b; Clark et al., 2013; Jokinen et al., 2012; Lee et al., 2009; Sundquist et al., 1983). Indeed, the presence of these peptides in the CSF at physiologically relevant concentrations suggests a potential role for volume transmission via the cerebroventricular system in the activation of extra-hypothalamic OXT-Rs. Furthermore, there is also evidence indicating that hypothalamic OXT-synthesizing neurons send direct axonal projections into many distant brain regions, including the hippocampus (Audigier and Barberis, 1985; Buijs and Swaab, 1979; Grinevich et al., 2016; Knobloch et al., 2012; Uvnas-Moberg et al., 2014; Zimmerman et al., 1984). Future studies using transgenic/optogenetic approaches may be able to more definitely determine the extent to which endogenous OXT and/or VP may drive inhibitory transmission in the dentate gyrus through activation of OXT-Rs, and may also be useful in further revealing and defining specific roles for intraventricular volume transmission, conventional synaptic transmission, and extrasynaptic signaling via axonally released peptides (e.g. see Landgraf and Neumann, 2004).

Finally, with respect to fully understanding the functional implications of OXT-R activation and the resultant GABA release in the dentate gyrus, we readily acknowledge there is much additional, and quite possibly exciting work left to be done. Local circuit neurons with similar intrinsic properties to those found in TGOT responsive hilar interneurons are found in several areas outside of the hilus (Markram et al., 2004). Like those described here, stuttering fast-spiking interneurons in other systems often demonstrate peri-threshold oscillations (Bracci et al., 2003). Such oscillations likely result from activation of an intrinsic voltage gated sodium conductance, and have been hypothesized to facilitate theta-frequency bursts of action potentials (Dorval and White, 2005). Through this type of

mechanism, activation of OXT-Rs in hilar interneurons may be involved in shaping spike timing in local excitatory circuits. Similarly, it is likely that TGOT responsive mossy cell targeting hilar interneurons participate in feedforward inhibition and help protect mossy cells from excitotoxicity. From that perspective, well timed activation of OXT-Rs could be neuroprotective, and help control runaway hyperexcitability that leads to epileptogenesis. Generally consistent with that idea, (Owen et al., 2013) demonstrated in CA1 that TGOT decreases spontaneous action potential firing of pyramidal neurons, however importantly, this phenomenon was also was observed concurrently with an increase in spike fidelity. Thus, it is also worth considering more subtle ways OXT-R activation in the hilus could selectively enhance or inhibit information flow early in the hippocampal trisynaptic circuit.

Supplementary Material

Refer to Web version on PubMed Central for supplementary material.

Acknowledgments

This work was supported by T90 DE021990-02 and R01 MH104641.

References

Acsady L, Katona I, Martinez-Guijarro FJ, Buzsaki G, Freund TF. Unusual target selectivity of perisomatic inhibitory cells in the hilar region of the rat hippocampus. J Neurosci. 2000; 20(18): 6907–19. [PubMed: 10995835]

Acsády L, Katona I, Martínez-Guijarro FJ, Buzsáki G, Freund TF. Unusual target selectivity of perisomatic inhibitory cells in the hilar region of the rat hippocampus. The Journal of neuroscience : the official journal of the Society for Neuroscience. 2000; 20(18):6907–19. [PubMed: 10995835]

Anagnostou E, Soorya L, Brian J, Dupuis A, Mankad D, Smile S, Jacob S. Intranasal oxytocin in the treatment of autism spectrum disorders: a review of literature and early safety and efficacy data in youth. Brain Res. 2014; 1580:188–98. [PubMed: 24508578]

Aoki Y, Yahata N, Watanabe T, Takano Y, Kawakubo Y, Kuwabara H, Iwashiro N, Natsubori T, Inoue H, Suga M, et al. Oxytocin improves behavioural and neural deficits in inferring others' social emotions in autism. Brain : a journal of neurology. 2014; 137(Pt 11):3073–86. [PubMed: 25149412]

Audigier S, Barberis C. Pharmacological characterization of two specific binding sites for neurohypophyseal hormones in hippocampal synaptic plasma membranes of the rat. The EMBO journal. 1985; 4(6):1407–12. [PubMed: 2992930]

Bartos M, Elgueta C. Functional characteristics of parvalbumin- and cholecystokinin-expressing basket cells. J Physiol. 2012; 590(Pt 4):669–81. [PubMed: 22250212]

Bean BP. The action potential in mammalian central neurons. Nat Rev Neurosci. 2007; 8(6):451–65. [PubMed: 17514198]

Beets I, Janssen T, Meelkop E, Temmerman L, Suetens N, Rademakers S, Jansen G, Schoofs L. Vasopressin/oxytocin-related signaling regulates gustatory associative learning in C. elegans. Science. 2012; 338(6106):543–5. [PubMed: 23112336]

Bracci E, Centonze D, Bernardi G, Calabresi P. Voltage-dependent membrane potential oscillations of rat striatal fast-spiking interneurons. J Physiol. 2003; 549(Pt 1):121–30. [PubMed: 12665602]

Buijs RM, Swaab DF. Immuno-electron microscopical demonstration of vasopressin and oxytocin synapses in the limbic system of the rat. Cell Tissue Res. 1979; 204(3):355–65. [PubMed: 527026]

Burton SD, Urban NN. Greater excitability and firing irregularity of tufted cells underlies distinct afferent-evoked activity of olfactory bulb mitral and tufted cells. J Physiol. 2014; 592(10):2097–118. [PubMed: 24614745]

Carson DS, Berquist SW, Trujillo TH, Garner JP, Hannah SL, Hyde SA, Sumiyoshi RD, Jackson LP, Moss JK, Strehlow MC, et al. Cerebrospinal fluid and plasma oxytocin concentrations are positively correlated and negatively predict anxiety in children. Mol Psychiatry. 2015a; 20(9): 1085–90. [PubMed: 25349162]

Carson DS, Garner JP, Hyde SA, Libove RA, Berquist SW, Hornbeak KB, Jackson LP, Sumiyoshi RD, Howerton CL, Hannah SL, et al. Arginine Vasopressin Is a Blood-Based Biomarker of Social Functioning in Children with Autism. PLoS One. 2015b; 10(7):e0132224. [PubMed: 26200852]

Chamberland S, Evstratova A, Toth K. Interplay between synchronization of multivesicular release and recruitment of additional release sites support short-term facilitation at hippocampal mossy fiber to CA3 pyramidal cells synapses. J Neurosci. 2014; 34(33):11032–47. [PubMed: 25122902]

Chapman CA, Lacaille JC. Intrinsic theta-frequency membrane potential oscillations in hippocampal CA1 interneurons of stratum lacunosum-moleculare. J Neurophysiol. 1999; 81(3):1296–307. [PubMed: 10085356]

Clark CL, St John N, Pasca AM, Hyde SA, Hornbeak K, Abramova M, Feldman H, Parker KJ, Penn AA. Neonatal CSF oxytocin levels are associated with parent report of infant soothability and sociability. Psychoneuroendocrinology. 2013; 38(7):1208–12. [PubMed: 23507187]

Dager SR, Wang L, Friedman SD, Shaw DW, Constantino JN, Artru AA, Dawson G, Csernansky JG. Shape mapping of the hippocampus in young children with autism spectrum disorder. AJNR Am J Neuroradiol. 2007; 28(4):672–7. [PubMed: 17416819]

Danglot L, Triller A, Marty S. The development of hippocampal interneurons in rodents. Hippocampus. 2006; 16(12):1032–60. [PubMed: 17094147]

Dorval AD Jr, White JA. Channel noise is essential for perithreshold oscillations in entorhinal stellate neurons. J Neurosci. 2005; 25(43):10025–8. [PubMed: 16251451]

Dumais KM, Veenema AH. Vasopressin and oxytocin receptor systems in the brain: Sex differences and sex-specific regulation of social behavior. Front Neuroendocrinol. 2015

Elgueta C, Kohler J, Bartos M. Persistent discharges in dentate gyrus perisoma-inhibiting interneurons require hyperpolarization-activated cyclic nucleotide-gated channel activation. J Neurosci. 2015; 35(10):4131–9. [PubMed: 25762660]

Feldman R, Golan O, Hirschler-Guttenberg Y, Ostfeld-Etzion S, Zagoory-Sharon O. Parent-child interaction and oxytocin production in pre-schoolers with autism spectrum disorder. Br J Psychiatry. 2014; 205(2):107–12. [PubMed: 24855128]

Freeman SM, Walum H, Inoue K, Smith AL, Goodman MM, Bales KL, Young LJ. Neuroanatomical distribution of oxytocin and vasopressin 1a receptors in the socially monogamous coppery titi monkey (Callicebus cupreus). Neuroscience. 2014; 273:12–23. [PubMed: 24814726]

Freund TF, Buzsaki G. Interneurons of the hippocampus. Hippocampus. 1996; 6(4):347–470. [PubMed: 8915675]

Fu LY, van den Pol AN. GABA excitation in mouse hilar neuropeptide Y neurons. J Physiol. 2007; 579(Pt 2):445–64. [PubMed: 17204505]

Gimpl G, Fahrenholz F. The oxytocin receptor system: structure, function, and regulation. Physiol Rev. 2001; 81(2):629–83. [PubMed: 11274341]

Gravati M, Busnelli M, Bulgheroni E, Reversi A, Spaiardi P, Parenti M, Toselli M, Chini B. Dual modulation of inward rectifier potassium currents in olfactory neuronal cells by promiscuous G protein coupling of the oxytocin receptor. J Neurochem. 2010; 114(5):1424–35. [PubMed: 20557424]

Grimmelikhuijzen CJ, Hauser F. Mini-review: the evolution of neuropeptide signaling. Regul Pept. 2012; 177(Suppl):S6–9. [PubMed: 22726357]

Grinevich V, Knobloch-Bollmann HS, Eliava M, Busnelli M, Chini B. Assembling the Puzzle: Pathways of Oxytocin Signaling in the Brain. Biol Psychiatry. 2016; 79(3):155–64. [PubMed: 26001309]

Hammock EA, Levitt P. Oxytocin receptor ligand binding in embryonic tissue and postnatal brain development of the C57BL/6J mouse. Front Behav Neurosci. 2013; 7:195. [PubMed: 24376405]

Hammock EA, Young LJ. Oxytocin, vasopressin and pair bonding: implications for autism. Philos Trans R Soc Lond B Biol Sci. 2006; 361(1476):2187–98. [PubMed: 17118932]

Hofmann ME, Bhatia C, Frazier CJ. Cannabinoid receptor agonists potentiate action potential-independent release of GABA in the dentate gyrus through a CB1 receptor-independent mechanism. J Physiol. 2011; 589(Pt 15):3801–21. [PubMed: 21646412]

Hollander E, Bartz J, Chaplin W, Phillips A, Sumner J, Soorya L, Anagnostou E, Wasserman S. Oxytocin increases retention of social cognition in autism. Biol Psychiatry. 2007; 61(4):498–503. [PubMed: 16904652]

Hollander E, Novotny S, Hanratty M, Yaffe R, DeCaria CM, Aronowitz BR, Mosovich S. Oxytocin infusion reduces repetitive behaviors in adults with autistic and Asperger's disorders. Neuropsychopharmacology. 2003; 28(1):193–8. [PubMed: 12496956]

Hosp JA, Struber M, Yanagawa Y, Obata K, Vida I, Jonas P, Bartos M. Morpho-physiological criteria divide dentate gyrus interneurons into classes. Hippocampus. 2014; 24(2):189–203. [PubMed: 24108530]

Hsu D. The dentate gyrus as a filter or gate: a look back and a look ahead. Prog Brain Res. 2007; 163:601–13. [PubMed: 17765740]

Insel TR, Hulihan TJ. A gender-specific mechanism for pair bonding: oxytocin and partner preference formation in monogamous voles. Behavioral neuroscience. 1995; 109(4):782–9. [PubMed: 7576222]

Insel TR, Shapiro LE. Oxytocin receptor distribution reflects social organization in monogamous and polygamous voles. Proc Natl Acad Sci U S A. 1992; 89(13):5981–5. [PubMed: 1321430]

Johnson ZV, Walum H, Jamal YA, Xiao Y, Keebaugh AC, Inoue K, Young LJ. Central oxytocin receptors mediate mating-induced partner preferences and enhance correlated activation across forebrain nuclei in male prairie voles. Horm Behav. 2015; 79:8–17. [PubMed: 26643557]

Jokinen J, Chatzittofis A, Hellstrom C, Nordstrom P, Uvnas-Moberg K, Asberg M. Low CSF oxytocin reflects high intent in suicide attempters. Psychoneuroendocrinology. 2012; 37(4):482–90. [PubMed: 21852050]

Joshi S, Hawken MJ. Loose-patch-juxtacellular recording in vivo--a method for functional characterization and labeling of neurons in macaque V1. J Neurosci Methods. 2006; 156(1–2):37–49. [PubMed: 16540174]

Knobloch HS, Charlet A, Hoffmann LC, Eliava M, Khrulev S, Cetin AH, Osten P, Schwarz MK, Seeburg PH, Stoop R, et al. Evoked axonal oxytocin release in the central amygdala attenuates fear response. Neuron. 2012; 73(3):553–66. [PubMed: 22325206]

Knobloch HS, Grinevich V. Evolution of oxytocin pathways in the brain of vertebrates. Front Behav Neurosci. 2014; 8:31. [PubMed: 24592219]

Kombian SB, Mouginot D, Pittman QJ. Dendritically released peptides act as retrograde modulators of afferent excitation in the supraoptic nucleus in vitro. Neuron. 1997; 19(4):903–12. [PubMed: 9354336]

Landgraf R, Neumann ID. Vasopressin and oxytocin release within the brain: a dynamic concept of multiple and variable modes of neuropeptide communication. Front Neuroendocrinol. 2004; 25(3–4):150–76. [PubMed: 15589267]

Larimer P, Strowbridge BW. Nonrandom local circuits in the dentate gyrus. J Neurosci. 2008; 28(47):12212–23. [PubMed: 19020015]

Lee R, Ferris C, Van de Kar LD, Coccaro EF. Cerebrospinal fluid oxytocin, life history of aggression, and personality disorder. Psychoneuroendocrinology. 2009; 34(10):1567–73. [PubMed: 19577376]

Leng G, Onaka T, Caquineau C, Sabatier N, Tobin VA, Takayanagi Y. Oxytocin and appetite. Progress in brain research. 2008; 170:137–51. [PubMed: 18655879]

Lerer E, Levi S, Salomon S, Darvasi A, Yirmiya N, Ebstein RP. Association between the oxytocin receptor (OXTR) gene and autism: relationship to Vineland Adaptive Behavior Scales and cognition. Mol Psychiatry. 2008; 13(10):980–8. [PubMed: 17893705]

Lindsly C, Frazier CJ. Two distinct and activity-dependent mechanisms contribute to autoreceptor-mediated inhibition of GABAergic afferents to hilar mossy cells. J Physiol. 2010; 588(Pt 15):2801–22. [PubMed: 20547680]

Lu W, Wen B, Zhang F, Wang JH. Voltage-independent sodium channels emerge for an expression of activity-induced spontaneous spikes in GABAergic neurons. Mol Brain. 2014; 7:38. [PubMed: 24886791]

Lubke J, Frotscher M, Spruston N. Specialized electrophysiological properties of anatomically identified neurons in the hilar region of the rat fascia dentata. J Neurophysiol. 1998; 79(3):1518–34. [PubMed: 9497429]

Ludwig M, Pittman QJ. Talking back: dendritic neurotransmitter release. Trends in neurosciences. 2003; 26(5):255–61. [PubMed: 12744842]

Lukas M, Bredewold R, Neumann ID, Veenema AH. Maternal separation interferes with developmental changes in brain vasopressin and oxytocin receptor binding in male rats. Neuropharmacology. 2010; 58(1):78–87. [PubMed: 19560475]

Maister L, Simons JS, Plaisted-Grant K. Executive functions are employed to process episodic and relational memories in children with autism spectrum disorders. Neuropsychology. 2013; 27(6): 615–27. [PubMed: 24245930]

Manning M, Misicka A, Olma A, Bankowski K, Stoev S, Chini B, Durroux T, Mouillac B, Corbani M, Guillon G. Oxytocin and vasopressin agonists and antagonists as research tools and potential therapeutics. J Neuroendocrinol. 2012; 24(4):609–28. [PubMed: 22375852]

Markram H, Toledo-Rodriguez M, Wang Y, Gupta A, Silberberg G, Wu C. Interneurons of the neocortical inhibitory system. Nat Rev Neurosci. 2004; 5(10):793–807. [PubMed: 15378039]

Modahl C, Green L, Fein D, Morris M, Waterhouse L, Feinstein C, Levin H. Plasma oxytocin levels in autistic children. Biol Psychiatry. 1998; 43(4):270–7. [PubMed: 9513736]

Mott DD, Turner DA, Okazaki MM, Lewis DV. Interneurons of the dentate-hilus border of the rat dentate gyrus: morphological and electrophysiological heterogeneity. J Neurosci. 1997; 17(11): 3990–4005. [PubMed: 9151716]

Muhlethaler M, Sawyer WH, Manning MM, Dreifuss JJ. Characterization of a uterine-type oxytocin receptor in the rat hippocampus. Proc Natl Acad Sci U S A. 1983; 80(21):6713–7. [PubMed: 6314337]

Nicolson R, DeVito TJ, Vidal CN, Sui Y, Hayashi KM, Drost DJ, Williamson PC, Rajakumar N, Toga AW, Thompson PM. Detection and mapping of hippocampal abnormalities in autism. Psychiatry Res. 2006; 148(1):11–21. [PubMed: 17056234]

Oh SW, Harris JA, Ng L, Winslow B, Cain N, Mihalas S, Wang Q, Lau C, Kuan L, Henry AM, et al. A mesoscale connectome of the mouse brain. Nature. 2014; 508(7495):207–14. [PubMed: 24695228]

Olazabal DE, Young LJ. Species and individual differences in juvenile female alloparental care are associated with oxytocin receptor density in the striatum and the lateral septum. Horm Behav. 2006; 49(5):681–7. [PubMed: 16442534]

Ophir AG, Gessel A, Zheng DJ, Phelps SM. Oxytocin receptor density is associated with male mating tactics and social monogamy. Horm Behav. 2012; 61(3):445–53. [PubMed: 22285648]

Owen SF, Tuncdemir SN, Bader PL, Tirko NN, Fishell G, Tsien RW. Oxytocin enhances hippocampal spike transmission by modulating fast-spiking interneurons. Nature. 2013; 500(7463):458–62. [PubMed: 23913275]

Porter JT, Cauli B, Staiger JF, Lambolez B, Rossier J, Audinat E. Properties of bipolar VIPergic interneurons and their excitation by pyramidal neurons in the rat neocortex. Eur J Neurosci. 1998; 10(12):3617–28. [PubMed: 9875341]

Prounis GS, Foley L, Rehman A, Ophir AG. Perinatal and juvenile social environments interact to shape cognitive behaviour and neural phenotype in prairie voles. Proceedings. Biological sciences / The Royal Society. 2015; 282(1819)

Raggenbass M, Tribollet E, Dubois-Dauphin M, Dreifuss JJ. Correlation between oxytocin neuronal sensitivity and oxytocin receptor binding: an electrophysiological and autoradiographical study comparing rat and guinea pig hippocampus. Proc Natl Acad Sci U S A. 1989; 86(2):750–4. [PubMed: 2536177]

Saitoh O, Karns CM, Courchesne E. Development of the hippocampal formation from 2 to 42 years: MRI evidence of smaller area dentata in autism. Brain. 2001; 124(Pt 7):1317–24. [PubMed: 11408327]

Sala M, Braida D, Lentini D, Busnelli M, Bulgheroni E, Capurro V, Finardi A, Donzelli A, Pattini L, Rubino T, et al. Pharmacologic rescue of impaired cognitive flexibility, social deficits, increased

aggression, and seizure susceptibility in oxytocin receptor null mice: a neurobehavioral model of autism. Biol Psychiatry. 2011; 69(9):875–82. [PubMed: 21306704]

Savanthrapadian S, Meyer T, Elgueta C, Booker SA, Vida I, Bartos M. Synaptic properties of SOM- and CCK-expressing cells in dentate gyrus interneuron networks. J Neurosci. 2014; 34(24):8197–209. [PubMed: 24920624]

Scharfman HE, Kunkel DD, Schwartzkroin PA. Intracellular dyes mask immunoreactivity of hippocampal interneurons. Neurosci Lett. 1989; 96(1):23–8. [PubMed: 2927710]

Sivukhina EV, Jirikowski GF. Magnocellular hypothalamic system and its interaction with the hypothalamo-pituitary-adrenal axis. Steroids. 2016

Spruston N, Lubke J, Frotscher M. Interneurons in the stratum lucidum of the rat hippocampus: an anatomical and electrophysiological characterization. J Comp Neurol. 1997; 385(3):427–40. [PubMed: 9300769]

Steinman MQ, Duque-Wilckens N, Greenberg GD, Hao R, Campi KL, Laredo SA, Laman-Maharg A, Manning CE, Doig IE, Lopez EM, et al. Sex-Specific Effects of Stress on Oxytocin Neurons Correspond With Responses to Intranasal Oxytocin. Biological psychiatry. 2015

Stoop R. Neuromodulation by oxytocin and vasopressin. Neuron. 2012; 76(1):142–59. [PubMed: 23040812]

Sundquist J, Forsling ML, Olsson JE, Akerlund M. Cerebrospinal fluid arginine vasopressin in degenerative disorders and other neurological diseases. J Neurol Neurosurg Psychiatry. 1983; 46(1):14–7. [PubMed: 6842195]

Taurines R, Schwenck C, Lyttwin B, Schecklmann M, Jans T, Reefschlager L, Geissler J, Gerlach M, Romanos M. Oxytocin plasma concentrations in children and adolescents with autism spectrum disorder: correlation with autistic symptomatology. Atten Defic Hyperact Disord. 2014; 6(3):231–9. [PubMed: 24989441]

Tepper JM, Tecuapetla F, Koos T, Ibanez-Sandoval O. Heterogeneity and diversity of striatal GABAergic interneurons. Front Neuroanat. 2010; 4:150. [PubMed: 21228905]

Tomizawa K, Iga N, Lu YF, Moriwaki A, Matsushita M, Li ST, Miyamoto O, Itano T, Matsui H. Oxytocin improves long-lasting spatial memory during motherhood through MAP kinase cascade. Nat Neurosci. 2003; 6(4):384–90. [PubMed: 12598900]

Tribollet E, Charpak S, Schmidt A, Dubois-Dauphin M, Dreifuss JJ. Appearance and transient expression of oxytocin receptors in fetal, infant, and peripubertal rat brain studied by autoradiography and electrophysiology. The Journal of neuroscience : the official journal of the Society for Neuroscience. 1989; 9(5):1764–73. [PubMed: 2542479]

Uvnas-Moberg K, Handlin L, Petersson M. Self-soothing behaviors with particular reference to oxytocin release induced by non-noxious sensory stimulation. Front Psychol. 2014; 5:1529. [PubMed: 25628581]

Viviani D, Terrettaz T, Magara F, Stoop R. Oxytocin enhances the inhibitory effects of diazepam in the rat central medial amygdala. Neuropharmacology. 2010; 58(1):62–8. [PubMed: 19589347]

von Engelhardt J, Eliava M, Meyer AH, Rozov A, Monyer H. Functional characterization of intrinsic cholinergic interneurons in the cortex. J Neurosci. 2007; 27(21):5633–42. [PubMed: 17522308]

Watanabe T, Abe O, Kuwabara H, Yahata N, Takano Y, Iwashiro N, Natsubori T, Aoki Y, Takao H, Kawakubo Y, et al. Mitigation of sociocommunicational deficits of autism through oxytocin-induced recovery of medial prefrontal activity: a randomized trial. JAMA psychiatry. 2014; 71(2): 166–75. [PubMed: 24352377]

Watanabe T, Kuroda M, Kuwabara H, Aoki Y, Iwashiro N, Tatsunobu N, Takao H, Nippashi Y, Kawakubo Y, Kunimatsu A, et al. Clinical and neural effects of six-week administration of oxytocin on core symptoms of autism. Brain : a journal of neurology. 2015; 138(Pt 11):3400–12. [PubMed: 26336909]

Zaninetti M, Raggenbass M. Oxytocin receptor agonists enhance inhibitory synaptic transmission in the rat hippocampus by activating interneurons in stratum pyramidale. Eur J Neurosci. 2000; 12(11):3975–84. [PubMed: 11069593]

Zhang L, Hernandez VS. Synaptic innervation to rat hippocampus by vasopressin-immuno-positive fibres from the hypothalamic supraoptic and paraventricular nuclei. Neuroscience. 2013; 228:139–62. [PubMed: 23085097]

Zimmerman EA, Nilaver G, Hou-Yu A, Silverman AJ. Vasopressinergic and oxytocinergic pathways in the central nervous system. Fed Proc. 1984; 43(1):91–6. [PubMed: 6690342]

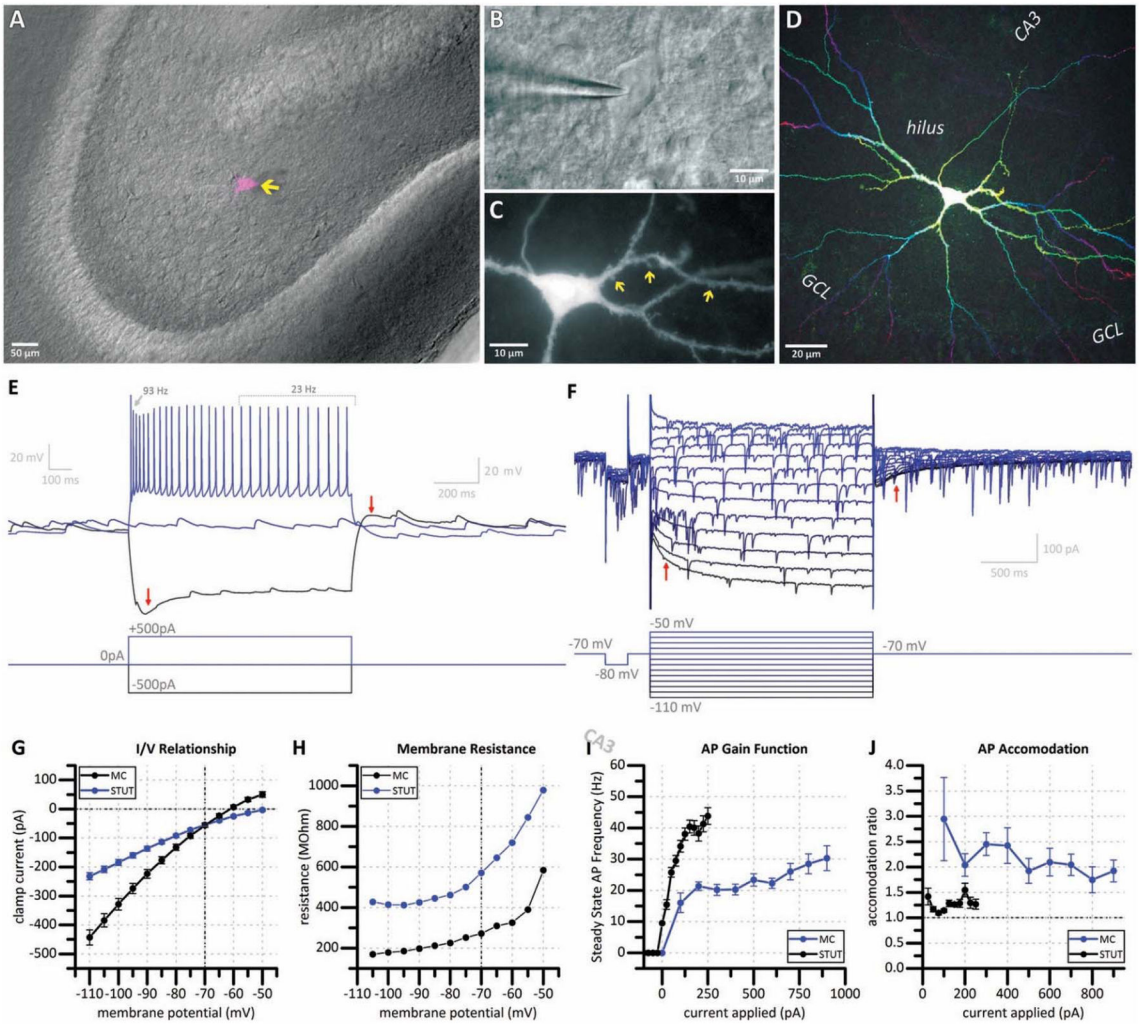

Figure 1. Morphological and electrophysiological identification of mossy cells

(a) Combined DIC (grayscale) and fluorescent (magenta) micrograph depicting a recorded hilar mossy cell (arrow). **(b)** DIC image of a representative mossy cell (asterisk) in whole-cell configuration. **(c)** Fluorescent micrograph of a biocytin-filled mossy cell reveals thorny excrescences (arrows) on proximal dendrites. **(d)** Depth-coded all-in-focus two-photon reconstruction of the same mossy cell reveals characteristic morphology. **(e)** Voltage traces (top) in response to increasing current steps (bottom) of a representative mossy cell. Mossy cells display a prominent sag current (left arrow) in response to a large hyperpolarizing current step, which is accompanied with a sustained depolarization for over one second (right arrow) following termination of the hyperpolarizing pulse. Mossy cells have a slow spiking and accommodating (accommodation ratio 4.0) firing pattern. **(f)** Current traces (top) in response to increasing voltage steps (bottom) reveals the same hyperpolarization activated excitatory current (left arrow) which persists for over one second (right arrow) following termination of the hyperpolarizing pulse. **(g)** Current / voltage relationship, **(h)** membrane resistance / voltage relationship, **(i)** action potential gain function, and **(j)**

accommodation ratio for all putative mossy cells recorded (MC) compared to non-mossy stuttering-type hilar interneurons (STUT).

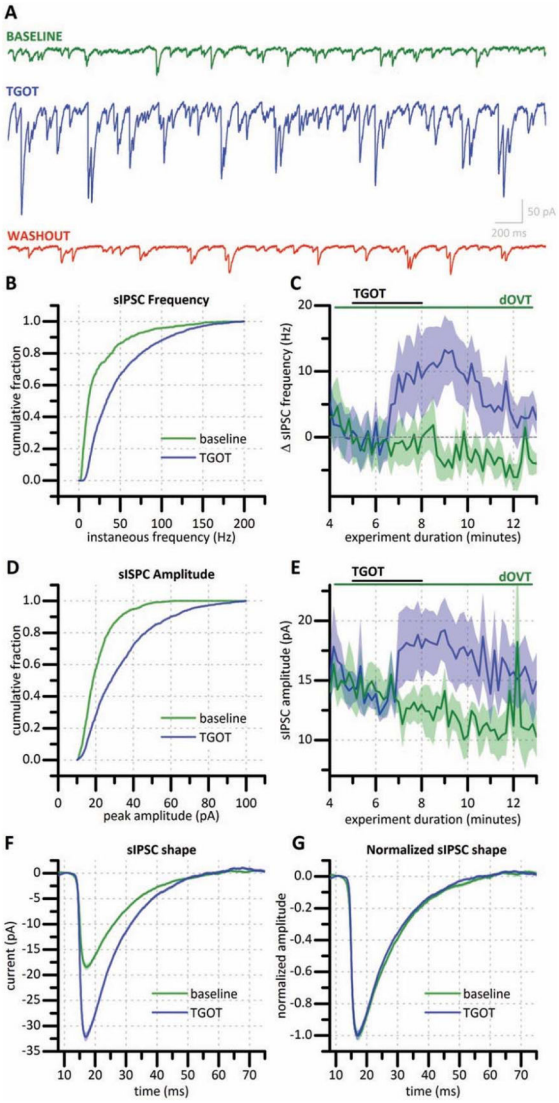

Figure 2. TGOT increases sIPSC frequency and amplitude in mossy cells

(a) Representative current traces from a mossy cell voltage clamped at −70 mV with a high Cl^- internal solution immediately before bath application of 200 nM TGOT (green trace), during maximum TGOT effect (blue trace), and 15 minutes following TGOT exposure (red trace). **(b)** Cumulative probability histogram showing instantaneous frequency for all sIPSCs recorded for two minutes before and two minutes following TGOT-exposure in a representative hilar mossy cell. **(c)** Change in sIPSC frequency produced by TGOT in the absence (blue trace, n=10) and presence (green trace, n=4) of dOVT, a selective OXT-R antagonist. **(d)** Cumulative probability histogram constructed using sIPSC amplitudes for all sIPSCs recorded for two minutes before and two minutes following TGOT-exposure in a representative hilar mossy cell. **(e)** Effect of TGOT on sIPSC amplitude averaged across 4 cells in the absence (blue trace) and presence (green trace) of dOVT. **(f)** Average sIPSC shape before drug application (green) and during TGOT exposure (blue) of a representative

mossy cell. **(g)** Average sIPSC normalized to peak amplitude. Traces in (c) and (e) indicate mean (solid line) +/− standard error (shaded region). [In C and E: blue n=10, green n=8]

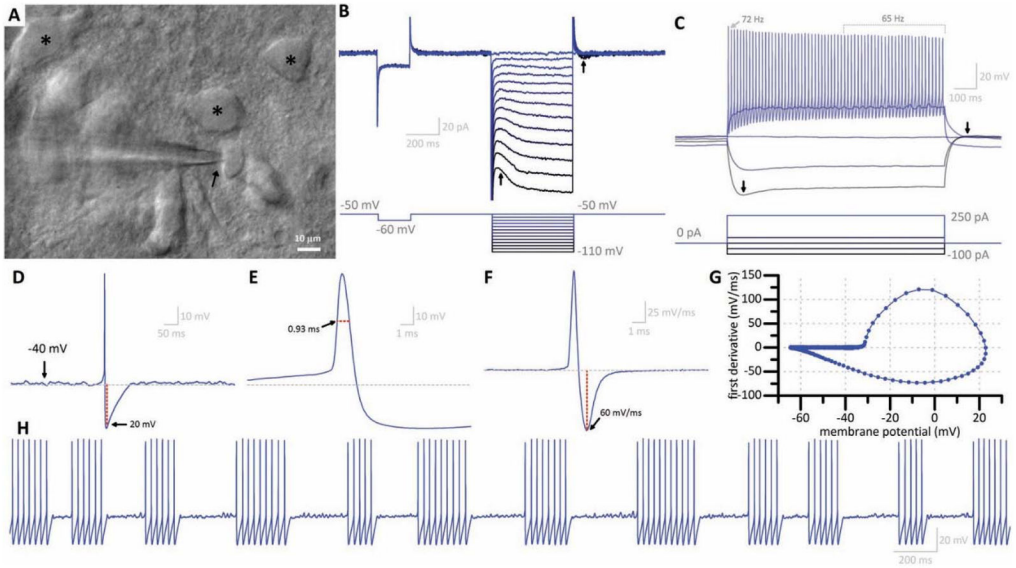

Figure 3. Common features of putative TGOT responsive hilar interneurons

(a) TGOT responsive hilar interneurons have small, smooth, ovoid soma as viewed under DIC optics (arrow) as compared to putative mossy cells (asterisks). **(b)** Current traces (top) in response to voltage steps (bottom) reveal a slowly-activating, quickly inactivating excitatory hyperpolarization-activated current (left arrow) which does not persist following return to resting voltage (right arrow). **(c)** Voltage traces (top) in response to current pulses (bottom) of a typical TGOT responsive hilar interneuron reveals this same current as a prominent sag (left arrow) but a rapid return to resting voltage (right arrow) following cessation of the current pulse. Peri-threshold oscillations are also frequently observed. TGOT responsive hilar interneurons are fast spiking (>40Hz steady state firing frequency) with little accommodation. **(d)** Spontaneous action potential of a TGOT responsive hilar interneuron reveals an AP threshold near −40 mV and a prominent afterhyperpolarization (AHP) of approximately 20 mV which persists for approximately 100 ms. Horizontal dotted line depicts average resting potential. **(e)** Magnified view of the action potential reveals a narrow half-width (defined as the time that the voltage exceeded the value observed halfway between threshold and peak).. **(f)** First-derivative of the action potential displays a characteristic large repolarization velocity (in excess of 60mV/ms). **(g)** Phase diagram combining data from (d) and (e). **(h)** Stuttering behavior of TGOT responsive hilar interneuron is elicited in response to +50pA continuous current injection. Perithreshold oscillations are visible between bursts of action potentials.

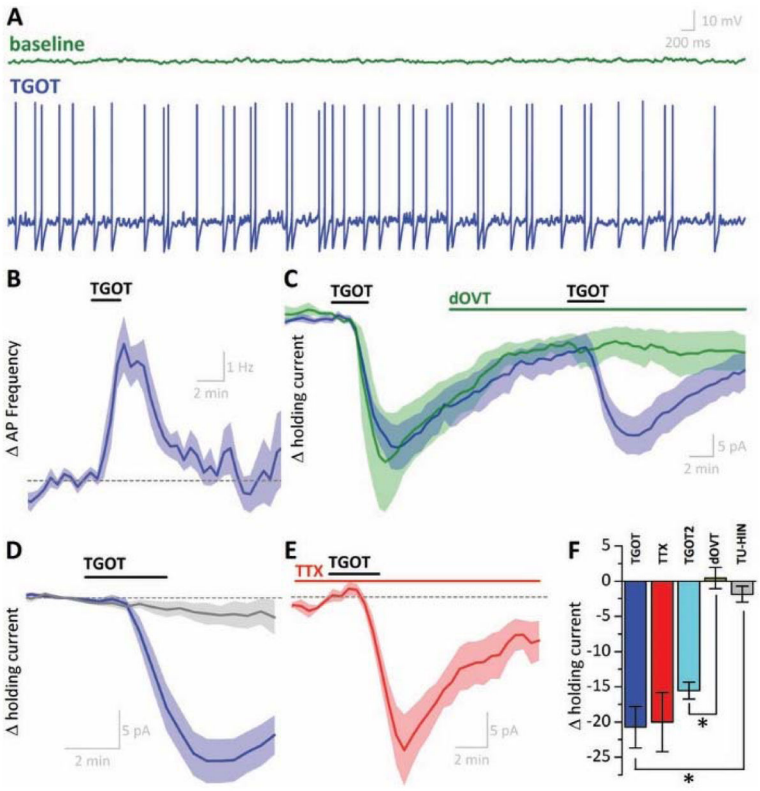

Figure 4. Excitatory nature of OXT-R activation in TGOT-responsive hilar interneurons ()

(a) Voltage trace of a representative TGOT responsive HILAR INTERNEURON. Brief TGOT exposure is sufficient to depolarize this cell from total quiescence (green) to a suprathreshold potential inducing continuous firing (blue, 60s later). **(b)** Average change in action potential (AP) frequency in all TGOT responsive hilar interneurons recorded in current-clamp mode. **(c)** In voltage clamp configuration, brief exposure to TGOT induces an excitatory current which can be repeated a second time following a 20 minute washout period (blue). In TGOT responsive hilar interneurons, application of dOVT completely abolishes response to subsequent application of TGOT (green). **(d)** Average current response of TGOT responsive hilar interneurons (blue, n=25) and TGOT unresponsive hilar interneurons (gray, n=14). **(e)** TGOT response occurs in the presence of tetrodotoxin (TTX). **(f)** Magnitude of TGOT response compared across experimental groups. TGOT: first TGOT exposure; TTX: first TGOT exposure in presence of TTX; TGOT2: second exposure of TGOT; dOVT: second exposure of TGOT in presence of dOVT; TU-HIN response of a TGOT unresponsive hilar interneuron. Data presented in panels B–E are baseline-subtracted to the 2-minute period prior to TGOT exposure. *$p < 0.05$

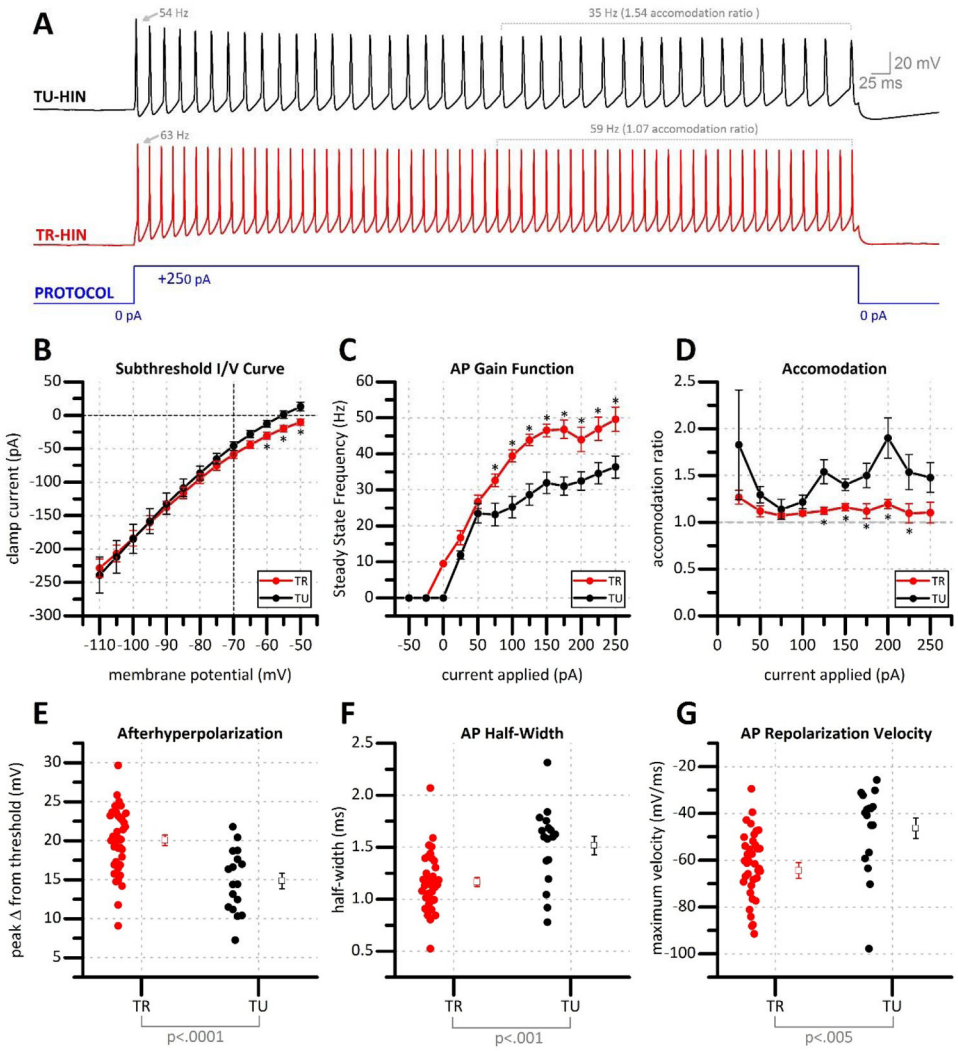

Figure 5. Comparison of electrophysiological properties of TR vs TU stuttering fast spiking hilar interneurons

(a) Stuttering hilar interneurons often fire regular trains of action potentials when depolarized by strong current injection (blue). In response to this stimulation paradigm, TGOT unresponsive hilar interneurons (TU-HIN, black) commonly present with spike accommodation. TGOT responsive hilar interneurons (TR-HIN, red) show little accommodation and demonstrate a higher steady state firing frequency in response to the same stimulus. **(b)** Steady state currents in response to a series of voltage steps in TGOT responsive (TR) and TGOT unresponsive (TU) hilar interneurons. **(c)** Action potential gain function and, **(d)** accommodation ratio in response to increasing current steps. Action potential **(e)** afterhyperpolarization magnitude, **(f)** half-width, and **(g)** repolarization velocity from TGOT responsive vs. TGOT unresponsive hilar interneurons. *p=<.05

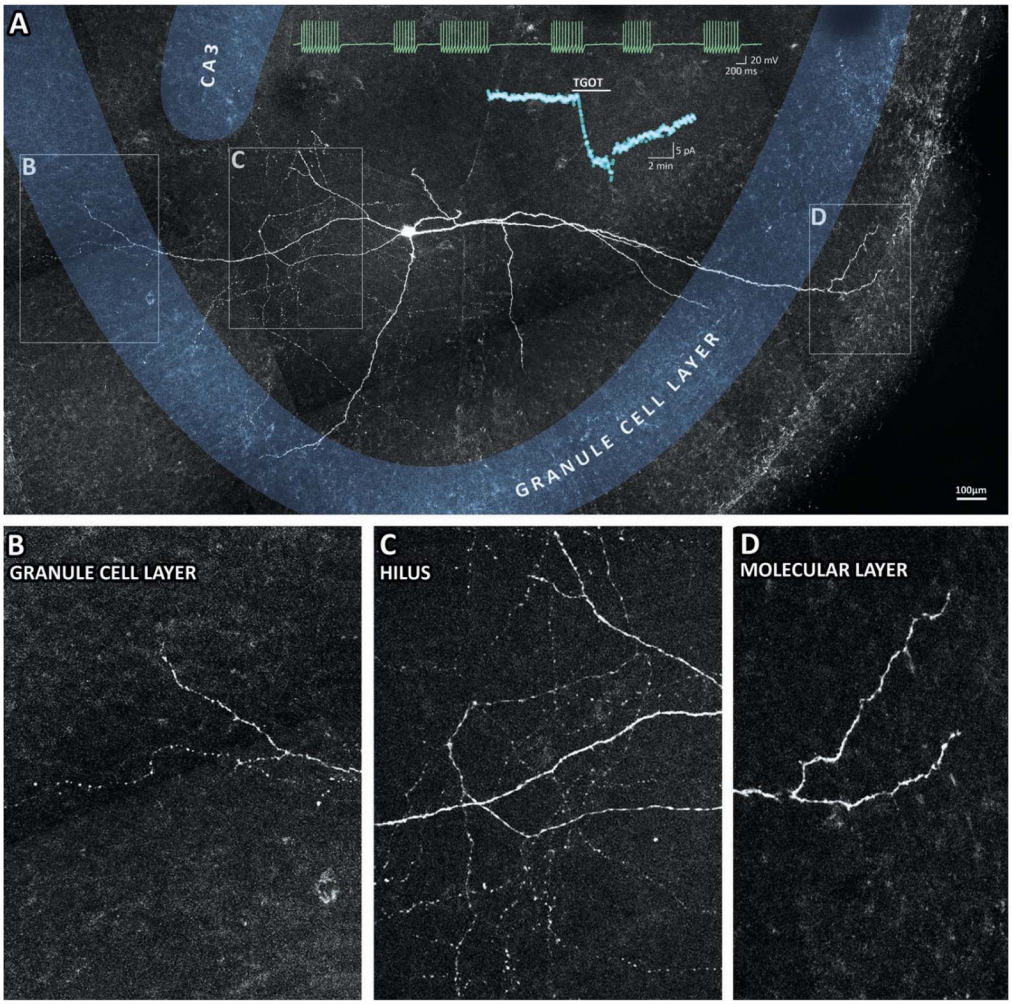

Figure 6. Morphology of typical TGOT-responsive fast-spiking interneuron

(a) Montage of multiple all-in-focus maximum-projection two-photon micrographs reveal a biocytin-filled TGOT responsive hilar interneuron neuron which exhibited typical stuttering firing behavior in current-clamp configuration (green inset) and a >20pA excitatory current in response to TGOT exposure in voltage-clamp configuration (cyan inset). Boxes in panel A highlight features of interest that are enlarged in panels B–D. Specifically, TGOT responsive hilar interneurons are often observed with axonal extensions which project to and beyond the granule cell layer **(b)** in addition to a dense network of varicose axons extending throughout the deep hilus **(c)**. Frequently TGOT responsive hilar interneurons are observed with a projecting dendrite which extends beyond the granule cell layer, and terminates in the outer molecular layer **(d)**.

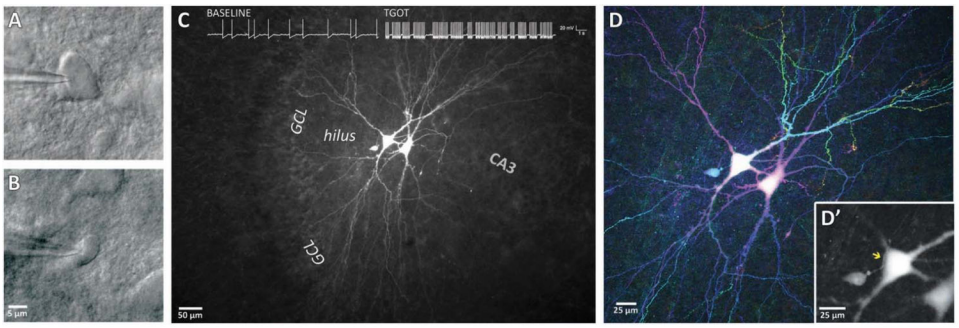

Figure 7. Anatomical Evidence of TGOT responsive hilar interneuron/mossy cell synapse

Hilar mossy cells were targeted for electrophysiological characterization in whole-cell configuration using DIC optics and filled with biocytin (A). Next, an adjacent stuttering hilar interneuron was targeted (B) and demonstrated to be TGOT responsive, as seen by an increase in action potential frequency following TGOT exposure (inset trace in C). Following histological labeling, 3D two-photon imaging (D) reveals detailed fine morphology of the large biocytin-filled mossy cells and the smaller TGOT responsive hilar interneuron, presented here as depth-coded maximum projection (with red/blue structures toward the surface of the slice, and green/yellow structures deeper in the tissue). A limited projection of 2 optical sections (D′) reveals a varicose axon from the TGOT responsive hilar interneuron (arrow) in close approximation with the soma and proximal dendrites of an adjacent mossy cell.